Open access • Journal Article • DOI:10.1016/0168-9002(92)90732-J

First results on the hybrid photodiode tube — Source link

R. DeSalvo, W. Hao, Y. You, Yaping Wang ...+1 more authors

Institutions: CERN

Published on: 01 May 1992 - Nuclear Instruments & Methods in Physics Research Section A-accelerators Spectrometers Detectors and Associated Equipment (North-Holland)

Topics: Detector, Semiconductor detector, Photodiode, Photocathode and Orders of magnitude (temperature)

EUROPEAN ORGANIZATION FOR NUCLEAR RESEARCH

CERN-LAA-HC/91-006
15th May 1991
CERN-PPE/91-142
15th May 1991

FIRST RESULTS ON THE HYBRID PHOTODIODE TUBE

R. DeSalvo[1], W. Hao[2]†, K. You[2]†, Y. Wang[2]†, C. Xu[2]†

[1] CERN - LAA Project, Geneva, Switzerland
[2] CERN - World Lab Fellow, Geneva, Switzerland

ABSTRACT

The performance of a new breed of light detectors based on a photocathode followed by a planar silicon diode working in the bombarding mode is reported. This detector was developed by the LAA project in order to produce a fast light detector capable of covering a span of the more than 4 orders of magnitude of linearity required by the scintillating fibre and lead ("spaghetti") calorimeter. Linear signals from single, to more than 10^6 photo-electrons per pulse were measured. The general characteristics of this detector are reported here.

(Submitted to Nuclear Instruments and Methods)

† On leave of absence from IHEP, Beijing, People's Republic of China.

INTRODUCTION

The Hybrid PhotoDiode (HPD) tube is made out of an ordinary photocathode mounted in front of a planar semiconductor diode (Si diode in the prototypes discussed here). The structure of the HPDs used in this test is shown in fig. 1.

The term HPD is a result of the fact that the photo-detector described consists of a vacuum diode containing a semiconductor diode. The photocathode and the diode at the anode are separated by a vacuum gap and are held at a potential difference of a few kilovolts. The semiconductor diode is biased to full depletion. The ohmic contact facing the photocathode is only a few hundred angstrom thick to allow for electron penetration.

An incoming photon is converted on the photocathode into a photoelectron, then accelerated and focussed towards the silicon diode by an electrostatic focusing system. The semiconductor diode is placed near the focal point of a spherical electric field and the photoelectrons are focused on a spot with an area of a few mm^2 on the chip. The accelerated photoelectrons stop in the depletion volume by generating electron-hole pairs. The gain obtained, equal to the number of electron-hole pairs created by a photoelectron inside the depleted volume of the silicon diode, is proportional to the photoelectron accelerating voltage. The collection of this charge produces the output current pulses of the hybrid photodiode tube.

For a period of time it was thought that one of us (R. D.) had been the first to conceptualize such a detector[1]. It was later realized that this principle of operation had already been investigated and set aside several times in the past[2] for reasons unknown to us. Despite the HPD's very interesting characteristics, there was never a large scale implementation of these devices.

A few prototypes of the HPD have been built for LAA with different electrostatic optics and semiconductor diode structures by DEP in Holland and by RTC-Philips in France. Tests on two types of HPD with equal electrostatic structure and the same type of silicon diode are reported here. These two HPD types differ in the orientation of the chip inside the tube (fig. 1b): in one case ("E" type) the chip is bombarded on the junction while in the other HPD ("T" type), photoelectrons enter the wafer from the back side of the diode. In both cases the ohmic contact is obtained by ion implantation and is very thin ($\sim$ few hundreds angstroms). A 75 μm thick 2 mm diameter silicon diode was mounted in the HPD used in the CERN tests.

In most of the tests described here, the HPD was excited with LEDs. Because of the low speed of the LED used at CERN (5 ns rise-time, several tens of ns fall-time depending on the signal amplitude) pulsed lasers were used to measure the HPD speed characteristics. The LED testing setup is described in fig. 2.

GAIN

The signal versus voltage curve of a HPD shows, as expected, a starting threshold of a few thousand Volts (corresponding to the minimum energy needed for the photo-electrons to cross the ohmic contact) followed by linear signal amplitude growth with the high voltage. Given the fact that just 3.6 eV are required to free an electron-hole

pair in a semiconductor, a gain of several thousand was expected at a working voltage of 10 kV. Typical gain curves are shown in fig. 3. The absolute gain was measured at DEP and Philips by comparing the HPD photocathode and output current and at CERN using the statistical fluctuations of the number of photons in a light pulse[3]. The linear gain behavior is particularly helpful in calorimetry because, unlike exponential gain devices, with the HPD a percentage of high voltage stability translates roughly into an equal percentage of gain stability.

The fact that the HPD works around 10 kV does not pose serious problems due to the fact that the HPD draws virtually no current and the high voltage can be produced locally with small, low power supplies developed for portable military image intensifiers.

The HPD silicon diodes need full depletion in order to work properly. The signal output of a "T" type HPD as a function of the silicon bias voltage was measured; at low bias voltage the signal obtained is small and shows very long tails. The tails were observed to disappear above the full depletion bias voltage. Integrated charge information on the charge collection was taken at the end of a lifetime test (fig. 4). Surprisingly, it was found that the integrated signal continues to increase well beyond the nominal full depletion voltage up to almost 100 Volts. It appears that the bias of 72 volts chosen at the beginning of the test is not adequate and that a bias of 100 V would have been a better choice for this diode. It was unclear if too low a bias voltage had mistakenly been chosen, or if a higher bias voltage is required due to ageing. In order to try to answer this question the signal versus high voltage curves at three different bias voltages were measured (fig. 5). It was found that the effect of the bias is concentrated under 10 kV on the threshold knee (fig. 5a), which is sharper for higher diode bias and softer for lower bias. The signal's increments with cathode high voltage are constant if the photocathode voltage is above 15 kV (fig. 5 b). It is believed that, initially, a bias voltage sufficient to sweep all the charge had been chosen, but that after ageing a higher bias is required. This point is further discussed in the chapter on ageing.

SPEED

Photon conversion in metal photocathodes has a time-scale of picoseconds or less and the photoelectron acceleration of a few kV in a spherical field has negligible time spread. The HPD speed is then limited by the semiconductor diode characteristics. Limiting factors are the capacity of the chip, the bias voltage, the contact resistance, the charge drift time inside the chip (2-3 ns) and the readout input resistance.

The speed of an "T" type HPD was measured with a 200 ps laser pulse in the laboratory of Dr. P. Benetti, INFN Pavia, Italy. The result is shown in fig. 6. Rise and fall times below 2 ns were obtained.

UNIFORMITY

Due to the spherical shape of the photocathode, photons enter it at different angles, thus experiencing different photon absorption thicknesses (but equal electron ejection thickness). A varying conversion efficiency is expected. The photoelectrons then enter the chip at different angles thus traversing different effective dead layer thicknesses and

experiencing different overall gains. These two effects work one against the other but it is not obvious that the HPD response will be flat across the photocathode. Tests were made with 1 millimetre diameter light pencils and typical results are shown in fig. 7. Uniformity variations of 5-10% were observed.

LINEARITY

The HPD electrostatic structure has virtually no space charge limitations and photocathode charging effects are negligible with photocathode voltages similar to a few kV. The planar silicon diodes have very large dynamic ranges. It was then expected, and consequently shown, that a very large signal dynamic range was possible.

HPD linearity was tested in the following way.

The HPDs were set up with four or more LEDs mounted in front of them. Light guides were used to couple the HPDs and LEDs in order to guarantee a uniform illumination (see fig. 2).

The driver of the first LED was tuned to have the highest possible signal amplitude, S_1, from the HPD.

The remaining LED drivers were adjusted so that HPD signal amplitudes were roughly in the following ratios:

$$S_1 = \text{A (arbitrary amplitude)}$$
$$S_2 = A/2 ,$$
$$S_3 = A/4 ,$$
$$S_4 = A/8 .$$

HPD signals were read out into a normal ADC (Lecroy 2249A) with a gate of about half a microsecond. The LED signals were first used individually and then fired in all possible combinations. The LED drivers shared the same power supply in order to avoid large driver loading effects. Whenever a LED driver was not used to excite a HPD it was loaded with an external LED.

Since, in a linear system, the signal read out in a given LED firing combination must be equal to the same combination of the individually read out signals, for all the LED combinations an "expected" signal was calibrated and plotted against the actual signal.

With four LEDs the linearity over almost one order of magnitude was explored. One or more ten-percent-transmittance neutral density filters were then inserted between the LEDs and the HPD to check the linearity in a different order of magnitude of the signal. External linear amplifiers or attenuators were used to fit output signals into the ADC active range.

This method was found to break down with very low signals because the LED's, driven with electrical pulses of up to 20 V, act as antennas and the picked up signals overwhelm the real one.

The results for a "T" type HPD are shown in fig. 8. The upper end scale of this curve corresponds to five million photoelectrons per pulse. To show with greater detail

the linearity of the HPD, percentage variations from the expected signal are shown in fig. 9.

In order to have enough light from the LED, the above measurements were performed with long pulses (50-100 ns). Faster light pulses can, in principle, cause saturation at lower integrated charge levels than in fig. 8 and 9. In a measurement from DEP in which the signal shape of an "E" type HPD was observed (fig. 10), no sign of saturation was found with 6 ns FWHM pulses and up to one hundred pC of charge output. Further study will be required in this direction.

HPD linearity at low light pulse intensity was studied in a different manner. A low noise charge amplifier[4] was mounted directly on the back of the HPD. The LED signal was attenuated and a gain measurement of the type described in Ref. 3 was performed. A constant slope (gain) from a single photon to the upper limit of the measurement (few thousand photons) was found (figs. 12 and 13). The induced pulses were not a problem in this measurement because the light output of the LED was changed by slightly altering the LED driver pulse height around the LED threshold.

SINGLE ELECTRON RESPONSE

The behaviour of the HPD with single photoelectrons was studied; an SER (Single photoElectron Response) pulse height spectrum is shown in fig. 13. The peaks of different numbers of photoelectrons are clearly separated. The observed SER width is essentially limited by electronics noise but some peak widening at large photoelectron numbers is visible. Theoretically, the HPD SER width should be roughly $1/\sqrt{G} \sim 2$ %. In practice, the SER width will also be limited by gain variations across the active surface. Even with all these limitations the HPD is obviously a good single photon counting device.

SHORT TERM STABILITY

To test the "T" HPD stability, 8 LEDs were set at high LED driver power and fired at 10 KHz. Output pulses were measured every few hours.

The first effect found was a 4-5% day to night signal variation due to response changes with room temperature. The thermal behaviour of the entire chain (LED drivers, LED, HPD and ADC) was measured and is shown in fig. 14a. The variations were roughly 1%/°C.

After the thermal variations were subtracted, a small linear signal decrease with time was observed and then tracked to the HPD ageing discussed below. After subtraction of this slope, the readout signal showed a residual variance of 0.12% over a period of four days (see fig. 15).

To disentangle the LED and readout chain thermal drifts from the HPD thermal characteristics, the HPD gain was measured as a function of temperature. Only the measurement black box was warmed with water. A preamplifier was also inside the box and its thermal behaviour was not factored out. Since this method measured only the gain, the photocathode efficiency variations (of the order of .3%/°C) were not visible. The results are shown in fig. 14b; no definite thermal effect was observed for the HPD gain.

LIFETIME

Both "E" and "T" type HPDs were tested for lifetime, exposing them to LED light flashes. An "E" type HPD was measured by DEP and a "T" type was measured at CERN. The measurement at CERN was done by stretching the short term stability test discussed above over several months and progressively increasing by a hundredfold, the light pulse frequency. In the DEP tests, the pulse amplitude was read out on a single pulse basis with an oscilloscope. At CERN the HPD integrated charge output was measured on an ADC, recording the average amplitude and variance of both signal and pedestal. Every few days the ageing measurement was interrupted to perform a fine grained gain versus voltage measurement. Both HPD types were tested at 10 kV photocathode voltage and both showed ageing but with drastically different characteristics.

The "E" type ageing curve is shown in fig. 16. It indicates a light output loss of 40% over 4000 hours (corresponding to an integrated output charge of almost 7 coulombs). The LED used in the ageing test was shined only on the central part of the photocathode and the ageing effect could be cross-checked by studying the photocathode uniformity curve. Indeed, a large decrease in signal was found in the centre of the HPD (see fig. 17); this effect was due to damage to the silicon. In fact, no effect was seen in the photocathode conversion efficiency measured in the charge collection mode (fig. 18). Much more worrisome was the effect found on the signal versus voltage curve (fig. 19a). This curve maintained its normal aspect in the undamaged outer ring while it showed a catastrophic change in the centre. Not only was signal diminished at the testing voltage of 10 kV but the gain for higher voltages flattens out, thus impeding gain recovery through a high voltage increase.

At first glance, the tests on the "T" type detector showed similar behaviour. The first thing found was a signal drop somewhat faster than for the "E" type. To compensate for this signal loss and in order to keep large signals in the ADC, the LED driver was returned several times during the measurement period. The signal pulse output versus the integrated output charge, normalized in order to take into account the LED retunings, is shown in fig. 20.

Gain versus voltage curves were then compared at different integrated output charges and it was discovered that they were changing shape in the 0 to 10 KV range while remaining linear beyond 10 kV (fig. 19b). This effect (different behaviour from fig. 19a to fig. 19b) was tentatively interpreted in the following way.

The photoelectrons used in the ageing tests penetrated the semiconductor for a distance $x = 3 \times 10^{-10} \times V^{1.4}$ cm, where x is about 1.2 μm at 10 kV. Probably, damage occurs in the form of defects that can stop the drifting charge. Obviously, the photoelectrons can produce damage only for the depth that they can penetrate. Also, the electron bombardment induced damage should be the same in both "T" and "E" HPD types because the diode substrate is the same.

Ageing was done with a 10 kV accelerating voltage. In the case of an "E" type HPD (fig. 19a), electron hole pairs converted deeper (than the 1.2 μm penetration of the 10 KeV photoelectrons) seemed to suffer the full damage while charge generated at

shallower subtrate depths was less affected. Conversely, in a "T" type HPD (fig. 19b), the damage affects only the charge converted at depths less than 1.2 μm. Since the two semiconductor diodes differ only in their drift field orientations, the observed effect is compatible with the concept of trapping being limited to the holes.

In the "E" type HPD, charge flows in the opposite direction. The holes freed at depths larger then 1.2 μm flow directly into the damaged volume and the situation is reversed. The gain versus voltage curve is only slightly changed if the photocathode voltage is less than 10 kV. Charge produced at depths greater than 1.2 μm by photoelectrons of more than 10 kV are fully attenuated, thus explaining the flattening of the gain curve. This interpretation is corroborated by observing, in fig. 5, that a sharper threshold knee is visible for higher bias voltage. This is to be expected since the recombination traps are less efficient with higher drift field inside the silicon.

The gain loss in a "T" type HPD can be recovered by increasing the photocathode high voltage. In the "E" type, the signal versus voltage curve saturates and the gain loss is unrecoverable.

It was also found that, due to LED efficiency loss, the actual gain loss was less than the apparent signal loss of fig. 20[5].

In the ageing test it would have been ideal to use a separate light detector to monitor the LEDs but a suitable light detector, more stable than the HPD under study, could not be found and consequently no monitor detector was used. As an alternative, the gain and the signal were output independently to disentangle the HPD from the LED ageing. Unfortunately, at the time of the ageing test the precision gain measurement technique of Ref. 3 had not yet been developed. Instead, the gain was estimated with the following two methods.

The signal versus voltage curves were taken with an unknown light pulse amplitude so that only their shape could be directly compared. Given the shape of the curves in fig. 19b and the above discussion, it was assumed that the ageing of the "T" type HPD was changing only the low voltage part of the curve. The signal versus voltage curves (the first and the last are shown in fig. 19b) were normalized so that all curves had the same slope in the 15 to 20 kV region. Signal amplitude was then measured at 10 kV and plotted in fig. 21a. This amplitude should be proportional only to the gain and not to the light pulse amplitude used in the gain measurement and was found to drop at half the rate of the signal of fig. 20.

Since, in all measurements, the signal, pedestal, variance of the signal σ_{signal} and the variance of the pedestal $\sigma_{\mathrm{pedestal}}$ were recorded, another measurement of the gain was obtained with the formula:

$$\mathrm{Gain} = \frac{\sigma^2_{\mathrm{signal}} - \sigma^2_{\mathrm{pedestal}}}{\mathrm{Signal} - \mathrm{Pedestal}} = \frac{\sigma^2}{\mathrm{S}} = \frac{(\sqrt{\mathrm{n_{pe}}}\mathrm{Gain})^2}{\mathrm{n_{pe}}\mathrm{Gain}}$$

This technique is related but statistically much coarser then the one in Ref. 3. In particular, it is subject to large fluctuations if $\sigma_{\mathrm{pedestal}}$ is too close to σ_{signal} (in fact in the first 2000 hours the gain was systematically overestimated due to poor detector electronics shielding). The result is shown in fig. 21b and is in good agreement with fig. 21a. Since these two methods are fully independent and in reasonable agreement with

each other, it is believed that the damage visible in fig. 20 is an overestimation and in part comes from LED ageing.

CONCLUSIONS

A new kind of light detector, termed the HPD, shows good performance in linearity, stability and speed. It can easily function as a single photon counter and its linear gain makes it particularly easy to use. Further development is necessary to increase the HPD lifetime but it is presently a useful device in many low light output tasks, including calorimetry. Since the photocathode is imaged on the silicon chip, by subdividing the silicon diode in pixels the HPD can become a position sensitive detector. The prototypes built so far rely on the fountain type, or on crossed focusing electrostatic optics and are not suitable for use in a magnetic field. The use of proximity focusing, as in the latest image intensifiers, will allow the HPD to be used in a magnetic field.

ACKNOWLEDGEMENTS

Most of the financial support for this project came from Consiglio Nazionale delle Ricerche, Italy. Financial contributions came also from DEP, Holland. The authors want to thank the staff of Camberra, DEP and RTC-Philips and in particular P. Burger at Camberra, A. Cochrane, R. Glazenborg, B. Van Geest and K. Stoop at DEP, M. Boutot, P. LHermite, M. Farrayre and J. Nussli at RTC-Philips for their enthusiastic work on this project. Thanks also goes to F. Hartjes at NIKHEF-H Amsterdam and P. Benetti of INFN-Pavia for performing the high speed measurements of the HPDs with their fast lasers. Finally R. D. desires to specially thank Prof. A. Zichichi, LAA Project Leader for his trust on what initially seemed a far fetched idea and for his support.

REFERENCES

[1] R. DeSalvo, *"Hybrid photo diode tube"*, CLNS 87-92, Cornell University, Ithaca, 1987; see also the proceedings of the 1987 Snowmass Workshop.

[2] R. Kalibjan, *"A phototube using 3 semiconductor diode as the multiplier element"*, IEEE Transactions on Nuclear Science, June 1966, p. 51.
J. M. Abraham et al., *"Application of solid-state elements to photoemissive devices"*, Advances in electronics and electron physics, p. 671, 1966.
P. Chevalier, *"Photomultiplicateur à haute résolution utilisant un multiplicateur semiconducteur"*, Nucl. Instr. and Meth. **50** (1967), 346-348.
J. Fertin. et al., *"Reverse epitaxial silicon diode for hybrid photomultiplier tube"*, IEEE Transactions of Nuclear Sciences vol. NS **15**, June 1968.
J.G. Cuby et al., preprint, *"High precision photometry, the electron bombarded diode approach"*, DAEC Observatoire de Meudon, Meudon, 1989.

[3] B. Bencheikh et al., *"A simple light detcctor gain measurement technique"*, CERN-LAA project, submitted to Nucl. Instr. and Meth., 1991.

[4] Charge amplifier prototype developed in the framework of the LAA project provided by P. Jarron, CERN.

[5] We were using the LED in a way not recommended from the constructor exciting them with 20 volts electrical pulses.

FIGURE CAPTIONS

Fig. 1. a) Schematic structure of one of the HPD tested; and b) the bombarded silicon diode structures.

Fig. 2. Block diagram of the testing apparatus for most of the HPD measurements reported here.

Fig. 3. HPD gain curve (Philips data) measured for an "E" type (circles) and for a "T" type (dots) diode.

Fig. 4. Signal output versus semiconductor diode bias voltage. Note that at low bias voltage the signal is not fully collected and a tail extends for hundreds of nanoseconds.

Fig. 5. Signal versus photocathode voltage plot at three different bias voltages. The measurement was made after the lifetime test. All the bias voltages are above the depletion voltage of 25 Volts: a) lower high voltage range, b) higher high voltage range.

Fig. 6. HPD pulse speed measurement. The HPD was excited by a 200 ps pulsed laser and read out on 50 Ω cable.

Fig. 7 a) Uniformity map of the response of a "T" type HPD (suppressed zero). b) Uniformity scan of the same HPD; the response is shown as open circles and the photocathode gain is in black dots. It is interesting to note that both measurements were made after several thousand hours of operation and more than ten coulomb of delivered signal.

Fig. 8. Measured versus expected charge from a "T" type HPD. The high (low) end corresponds to about 5 million (300) photoelectrons per pulse.

Fig. 9. Plot of percentage variations from the expected charge versus measured charge.

Fig. 10. Pulse recorded from an "E" type HPD (100 V bias) excited by an LRZ 181 fast LED and read out on 25 Ω load. DEP measurement.

Fig. 11. The square of the variance of the signals is plotted versus the pulse height of the signals for various LED light pulse levels. Light pulses range from less than one photoelectron/pulse up to 3000 photoelectrons/pulse. The measurement was divided into two pieces to fit in the ADC range: a) an external amplifier was used; b) an external attenuator was used. The slope is proportional to the amplifier gain. Both curves are linear showing constant gain.

Fig. 12. From the data of fig. 11 the number of photoelectrons per pulse was calculated and plotted against the recorded signal.

Fig. 13. Response spectrum of an HPD to few photoelectron pulses. The ADC pedestal is also shown.

Fig. 14. a) Thermal behaviour of the LED driver, LED, HPD, and ADC chain. The measurement was made taking advantage of the laboratory thermal excursion. b) Normalized HPD gain versus temperature; the measurement includes the thermal variation of a charge preamplifier.

Fig. 15. HPD signal variations after thermal and ageing corrections. A variance of 0.12% over four days is observed.

Fig. 16. HPD ("E" type) pulse height versus ageing time; the HPD was excited and aged with a pulsed HLMP3750 LED illuminating the central part of the photocathode. The pulse frequency was 10 KHz (DEP data).

Fig. 17. HPD ("E" type) response versus active surface position measured after ageing. Clear degradation is visible in the central part where the LED was shining (DEP data).

Fig. 18. Photocathode scan of the same HPD of fig. 15 before (a) and after (b) ageing. The solid line is a vertical photocathode scan, the dashed line a horizontal scan. No damage is visible and all the performance degradation is attributed to damage to the silicon diode (DEP data).

Fig. 19. Gain versus voltage curve for: "E" type (a.) (DEP data); and "T" type (b.) (CERN data) HPDs. For the "E" type HPD a signal versus voltage scan is measured first shining the light source on the border region of the HPD photocathode (undamaged, black circles) and then on the centre (damaged, open circles) For the "T" type a signal versus voltage scan is taken before (black circles) and after (open circles) ageing.

Fig. 20. Signal loss of a "T" type HPD versus the delivered charge. Note the suppressed scale. Part of the signal loss was then attributed to the LED or photocathode ageing.

Fig. 21. Two different gain measurements performed throughout the ageing test are plotted versus the integrated charge delivered by the "T" type HPD. a) The signal normalization is obtained by equalizing the gain increments in the undamaged regione between 15 and 20 kV. The signal at 10 kV is proportional to the gain. b) The gain measurement is obtained by studying the statistical fluctuations of the light pulses.

a)

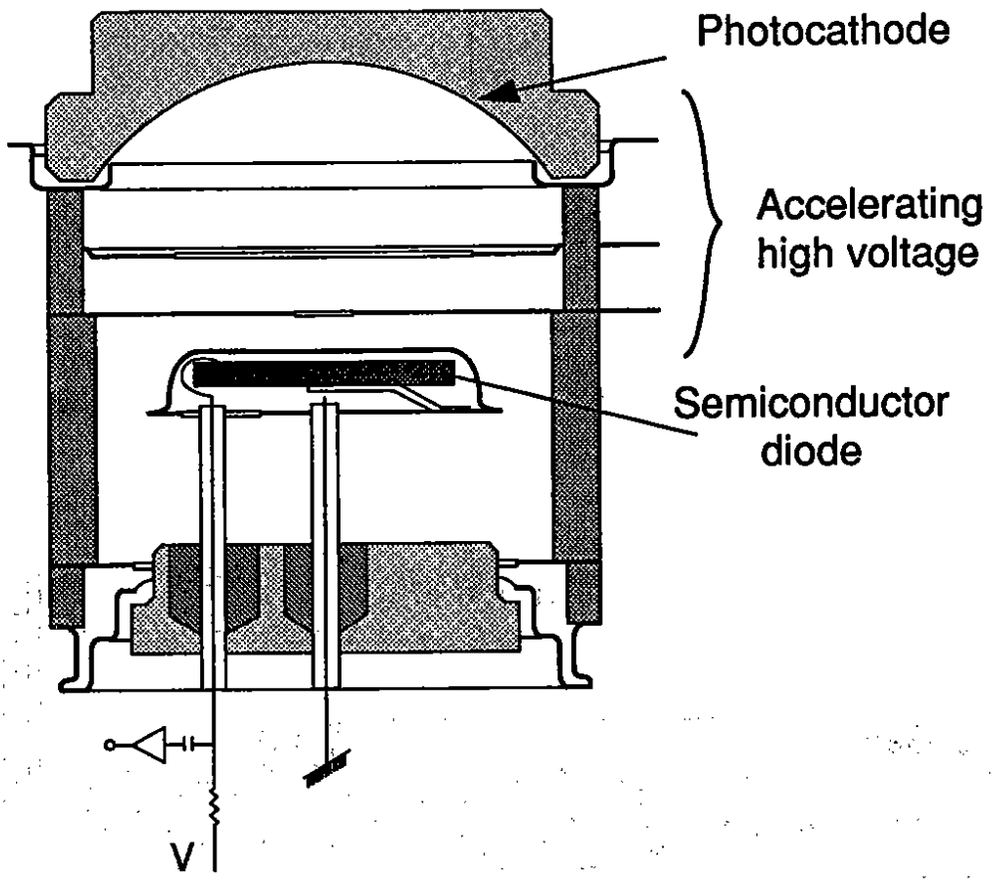
Photocathode
Accelerating high voltage
Semiconductor diode
V

b)

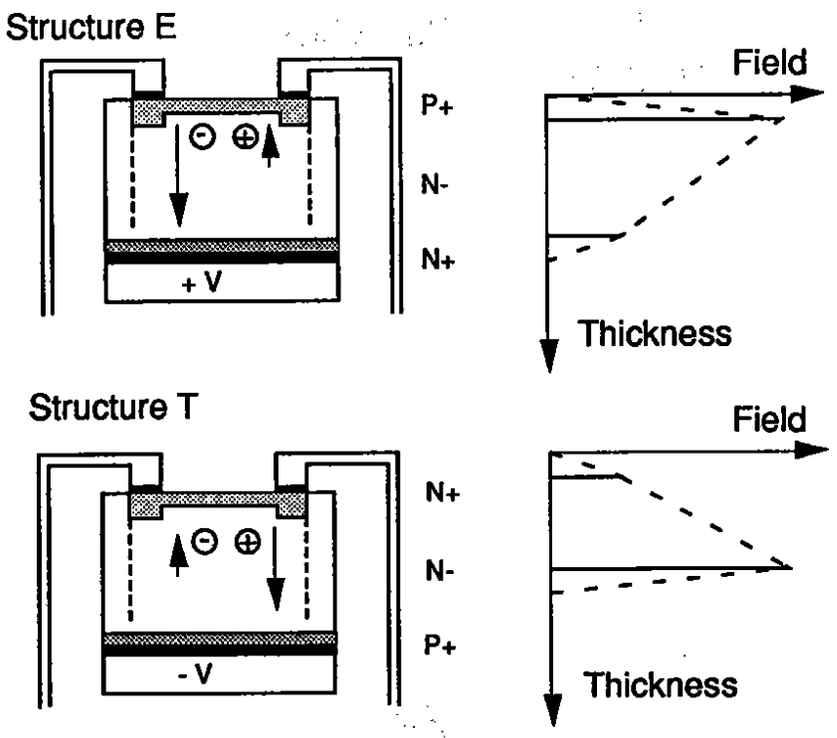
Structure E
P+
N-
N+
+ V
Field
Thickness
Structure T
N+
N-
P+
- V
Field
Thickness

Fig. 1.

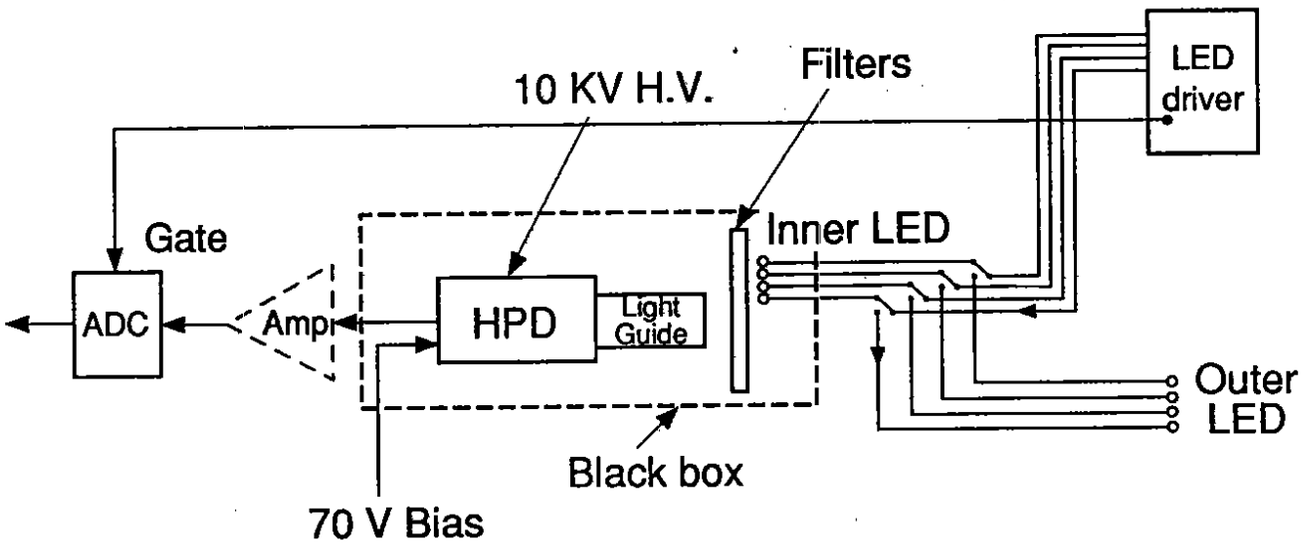
LED
driver
10 KV H.V.
Filters
Gate
Inner LED
ADC
Amp
HPD
Light
Guide
Outer
LED
Black box
70 V Bias

Fig. 2.

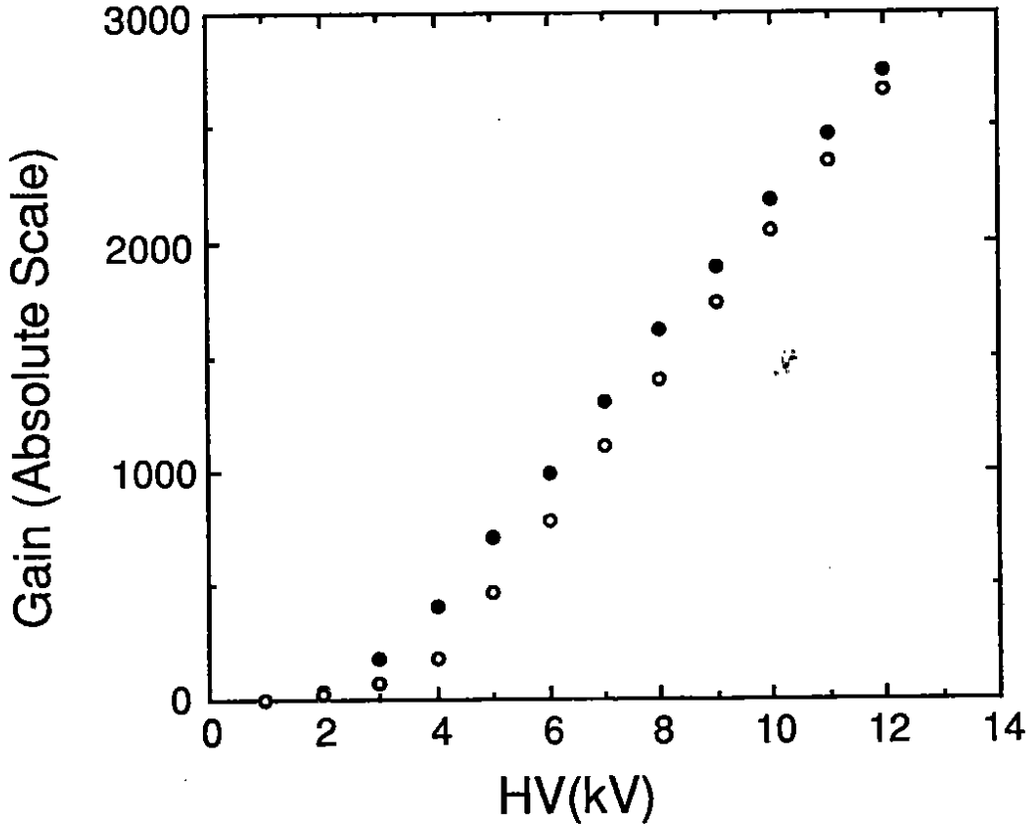

Fig. 3.

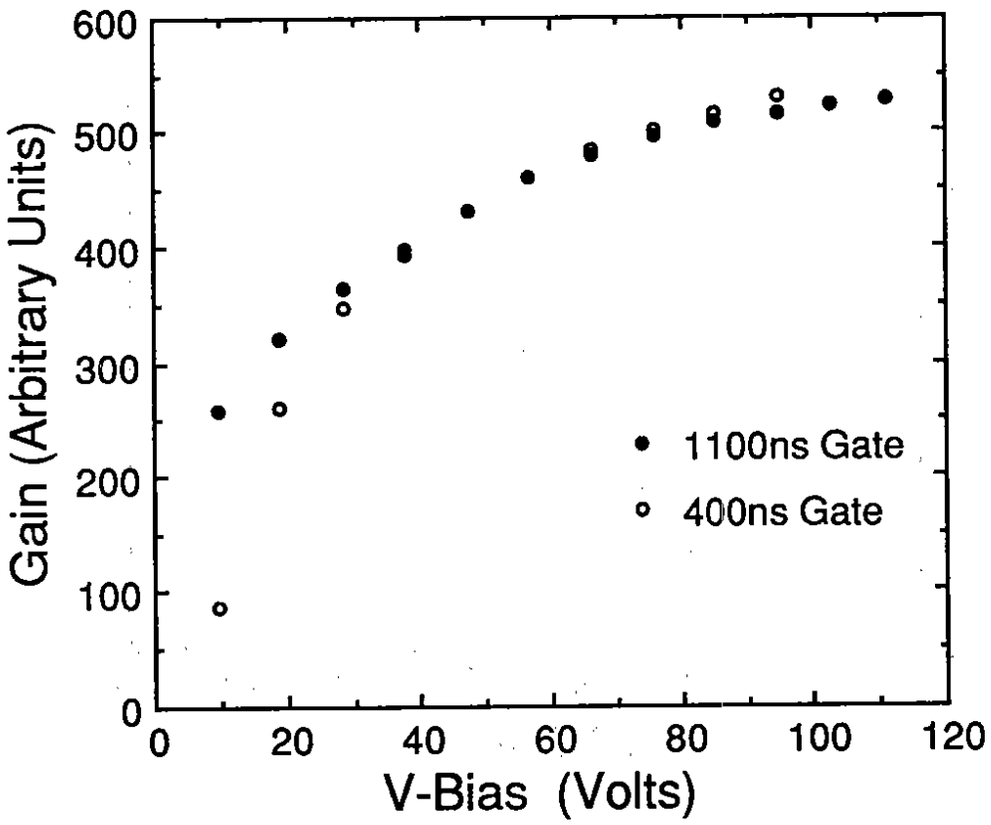
600
500
400
300
200
100
0
Gain (Arbitrary Units)
0
20
40
60
80
100
120
V-Bias (Volts)
1100ns Gate
400ns Gate

Fig. 4.

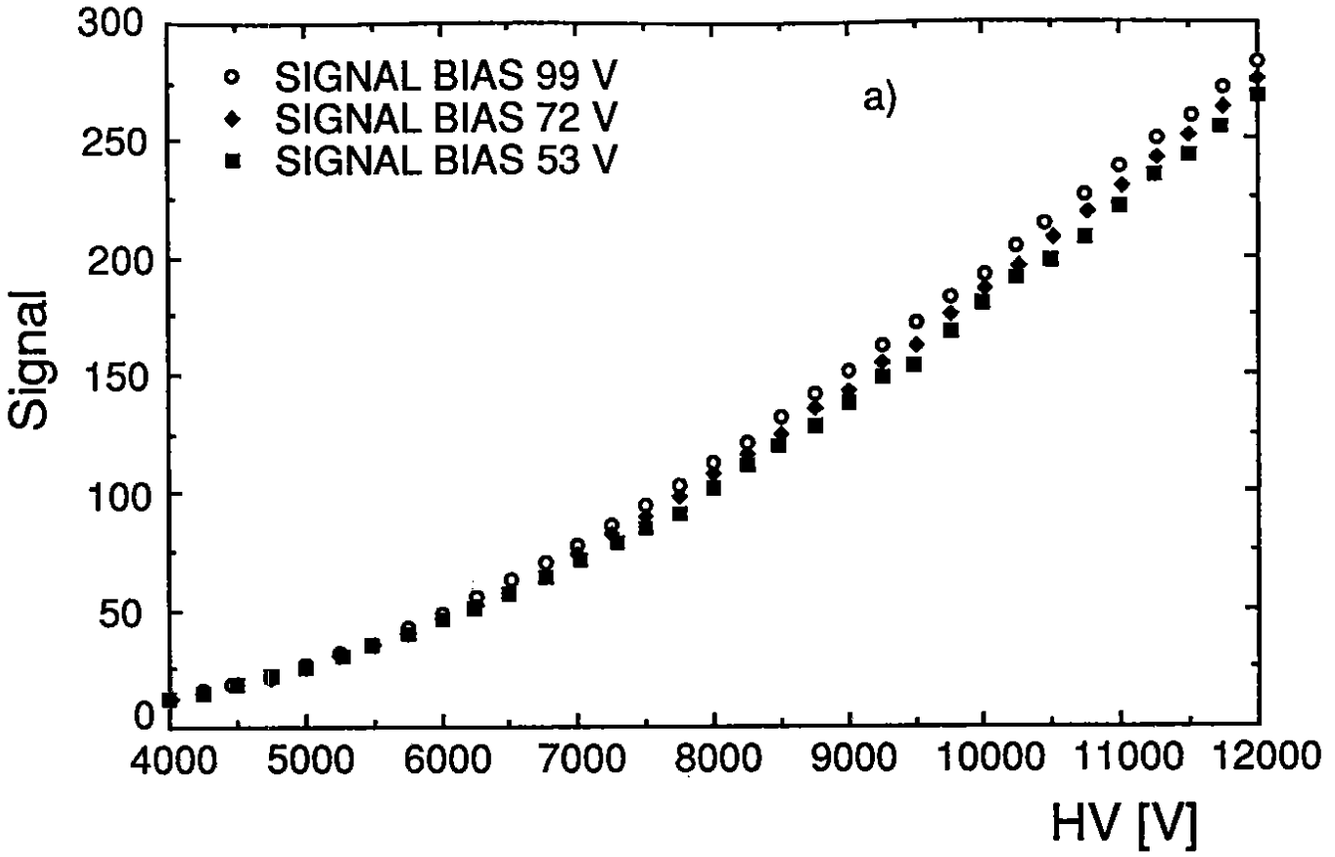
SIGNAL BIAS 99 V
SIGNAL BIAS 72 V
SIGNAL BIAS 53 V
a)
Signal
HV [V]
300
250
200
150
100
50
0
4000
5000
6000
7000
8000
9000
10000
11000
12000

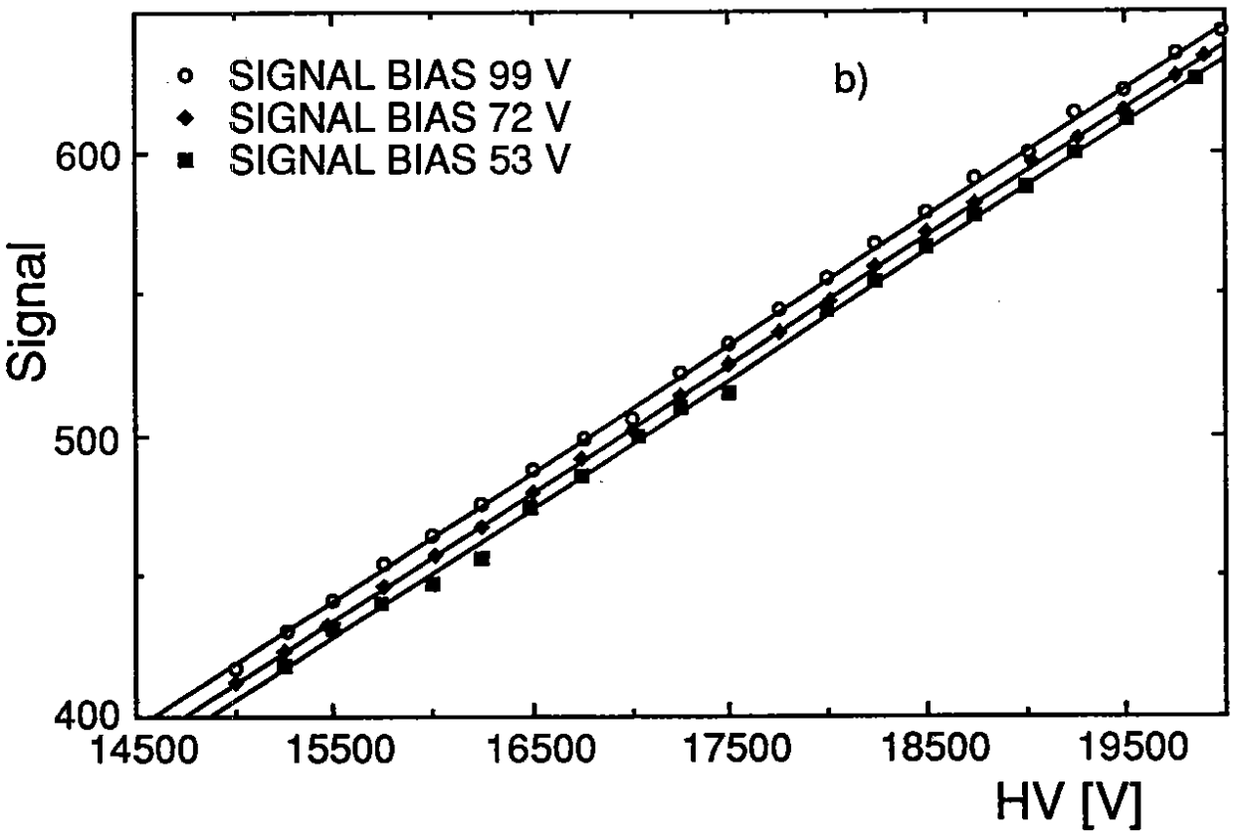
SIGNAL BIAS 99 V
SIGNAL BIAS 72 V
SIGNAL BIAS 53 V
b)
Signal
HV [V]
600
500
400
14500
15500
16500
17500
18500
19500

Fig. 5.

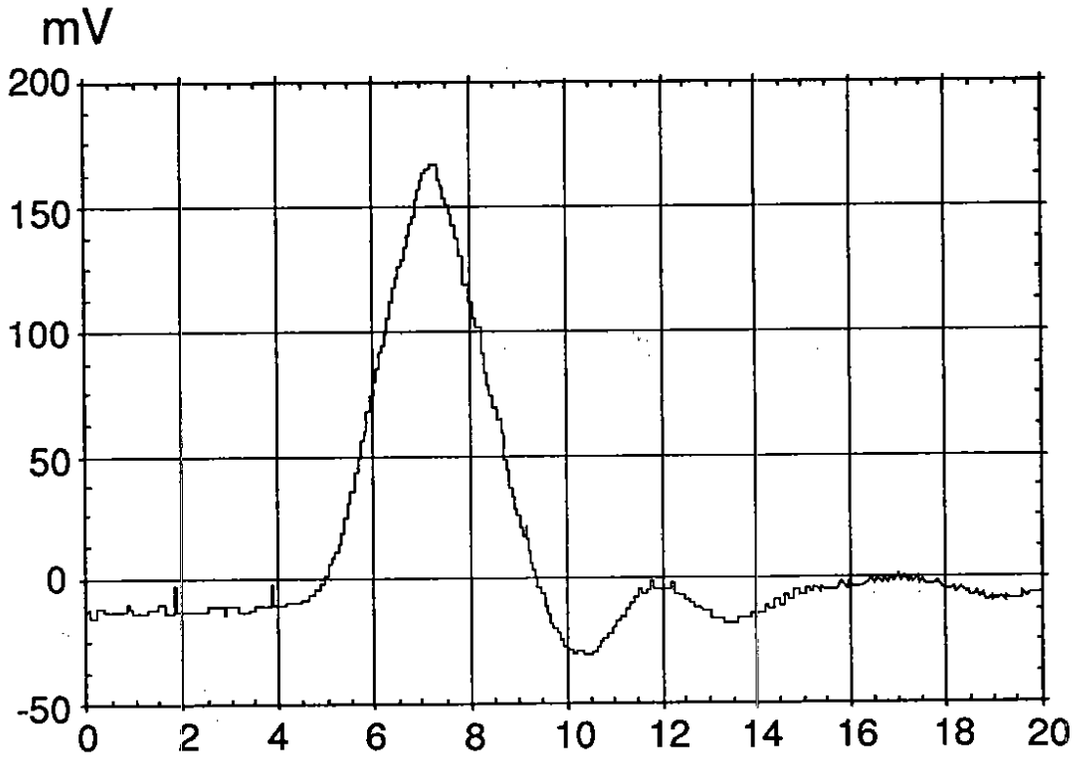

Fig. 6.

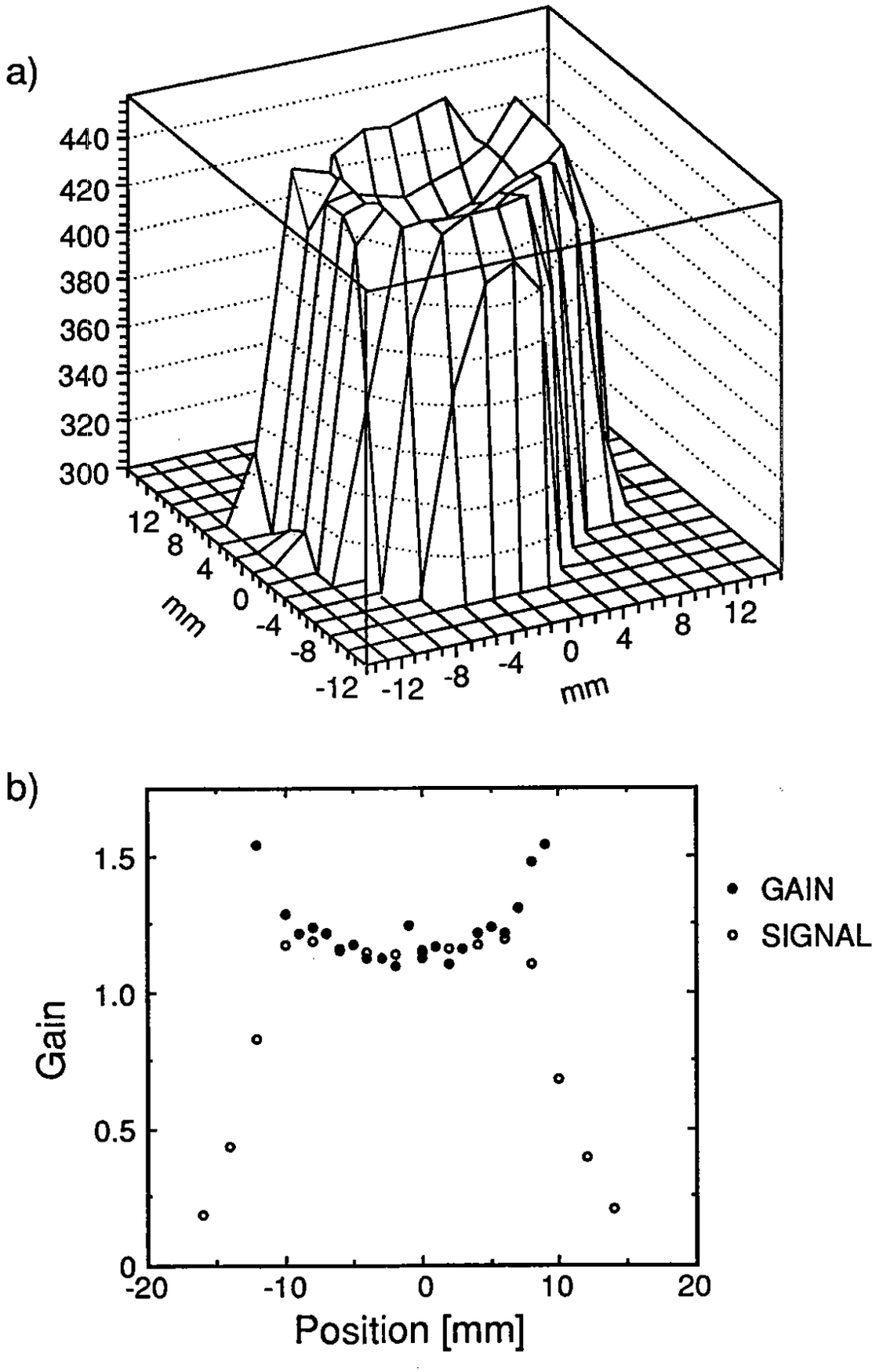
a)
440
420
400
380
360
340
320
300
12
8
4
0
-4
-8
-12
mm
-12
-8
-4
0
4
8
12
mm
b)
1.5
1.0
0.5
0
Gain
-20
-10
0
10
20
Position [mm]
GAIN
SIGNAL

Fig. 7.

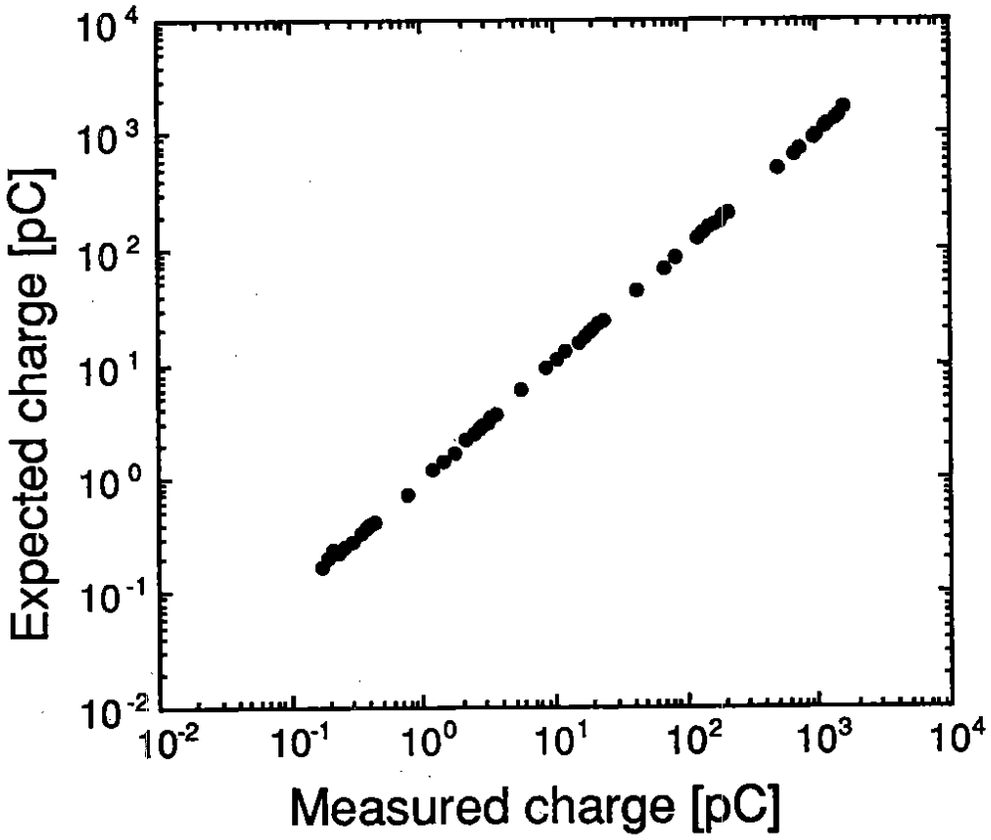
Expected charge [pC]
Measured charge [pC]
10^4
10^3
10^2
10^1
10^0
10^-1
10^-2
10^-2
10^-1
10^0
10^1
10^2
10^3
10^4

Fig. 8.

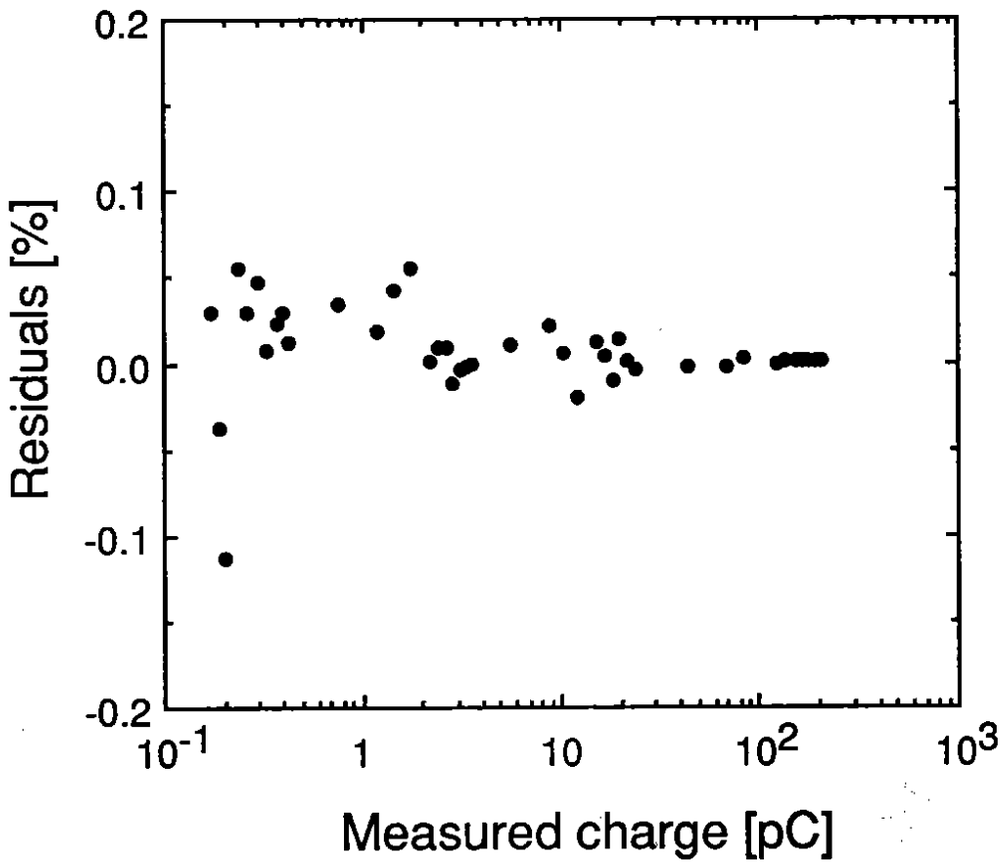

Fig. 9.

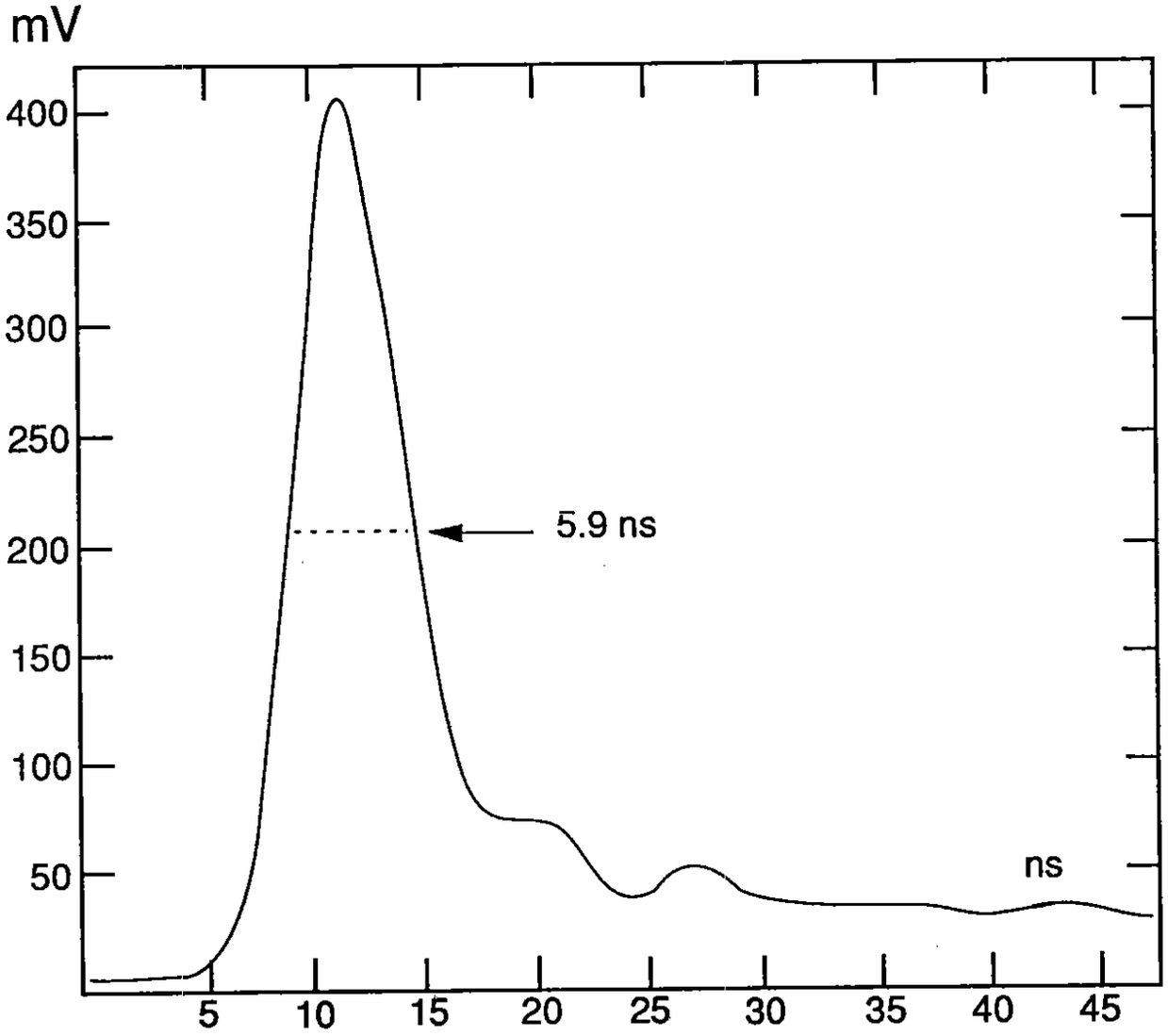

Fig. 10.

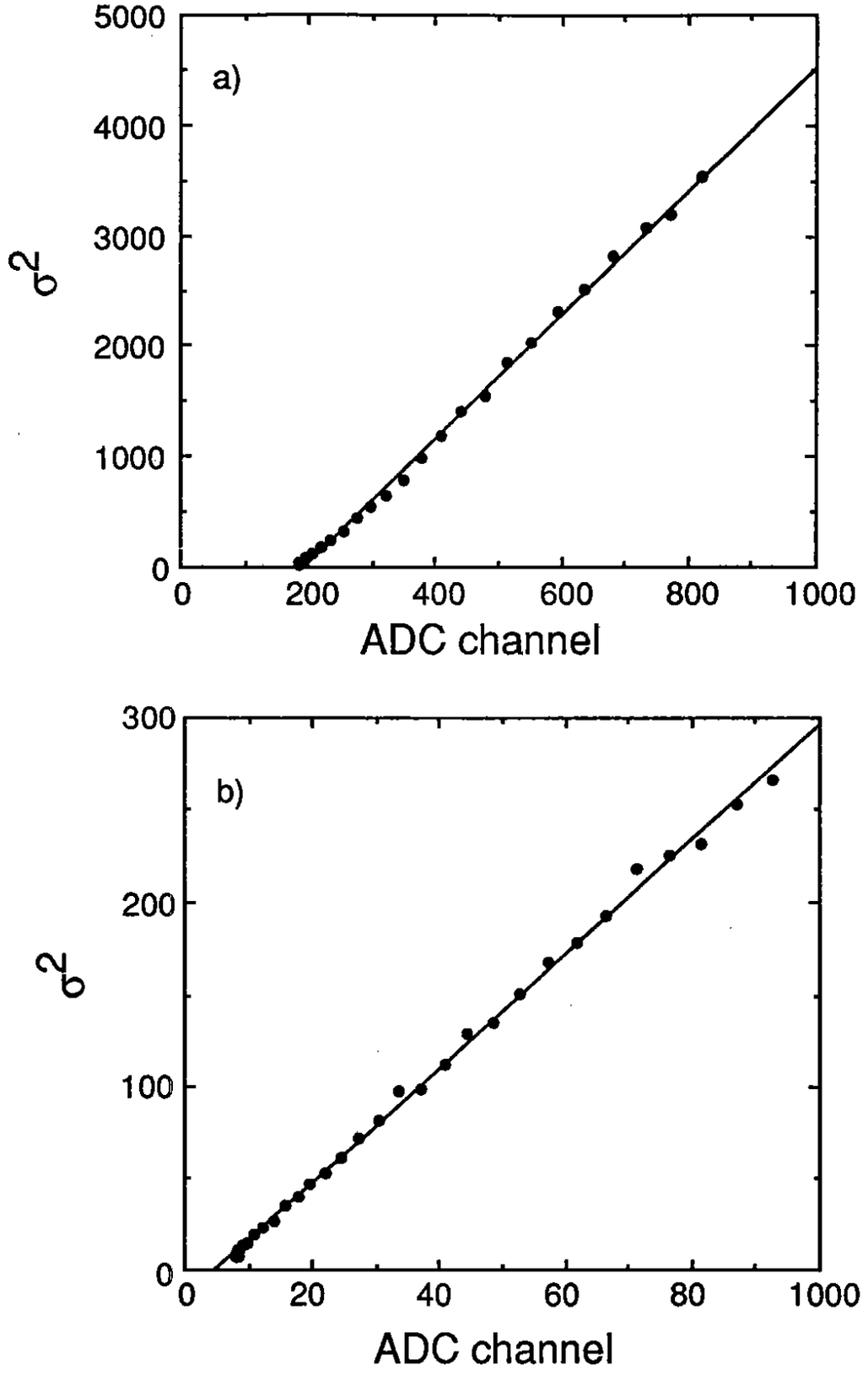
a)
5000
4000
3000
2000
1000
0
σ2
0
200
400
600
800
1000
ADC channel
b)
300
200
100
0
σ2
0
20
40
60
80
1000
ADC channel

Fig. 11.

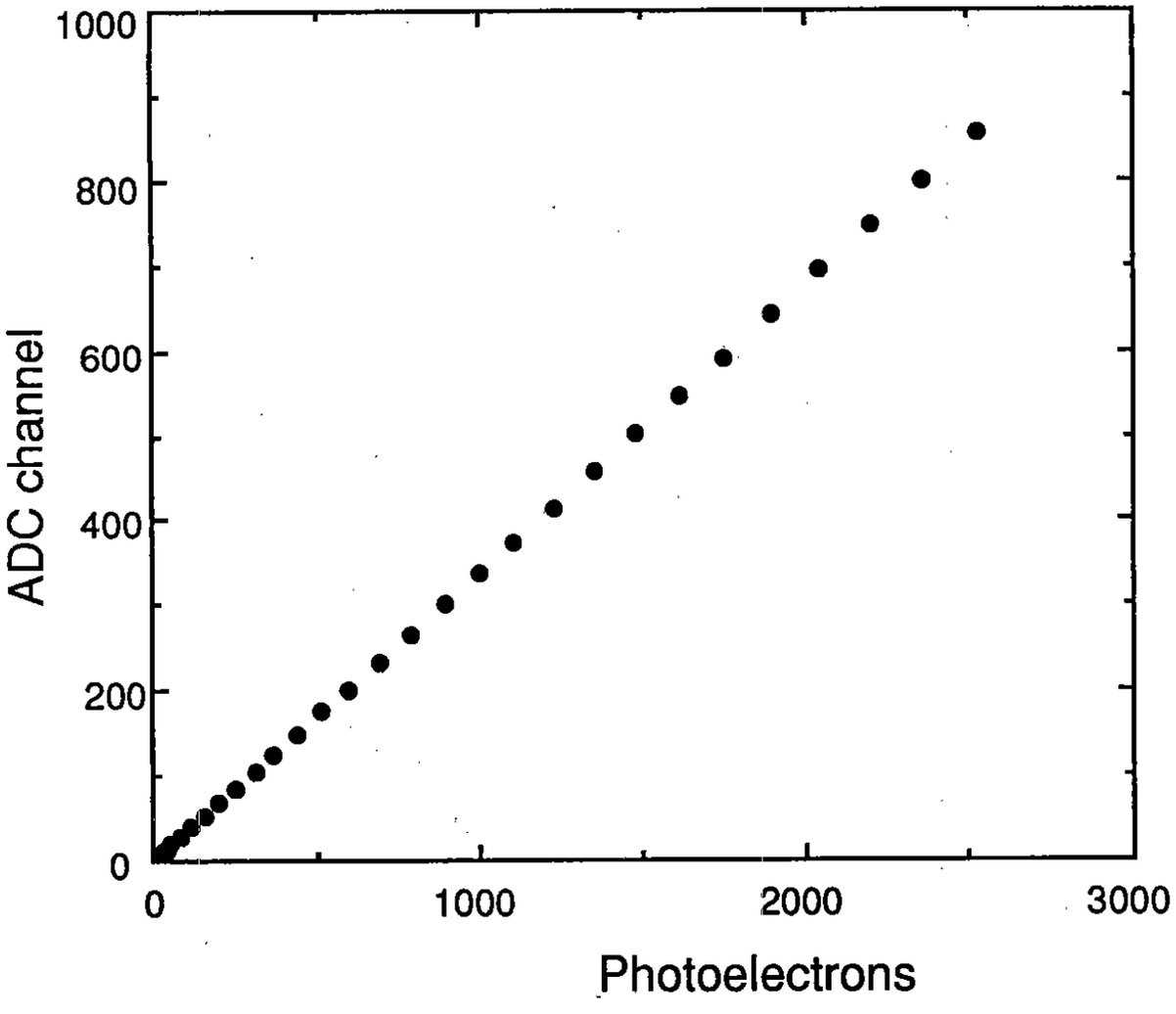
1000
800
600
400
200
0
ADC channel
0
1000
2000
3000
Photoelectrons

Fig. 12.

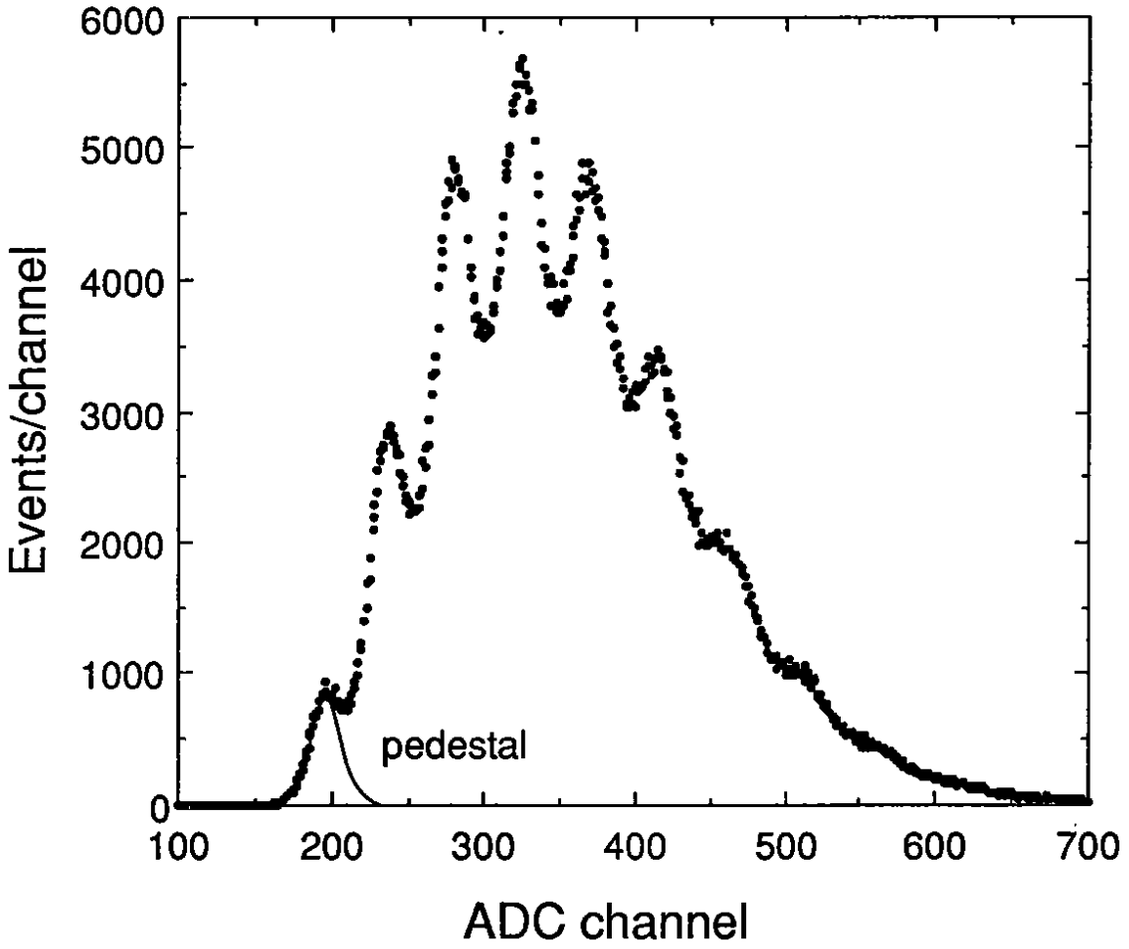
6000
5000
4000
3000
2000
1000
0
Events/channel
pedestal
100
200
300
400
500
600
700
ADC channel

Fig. 13.

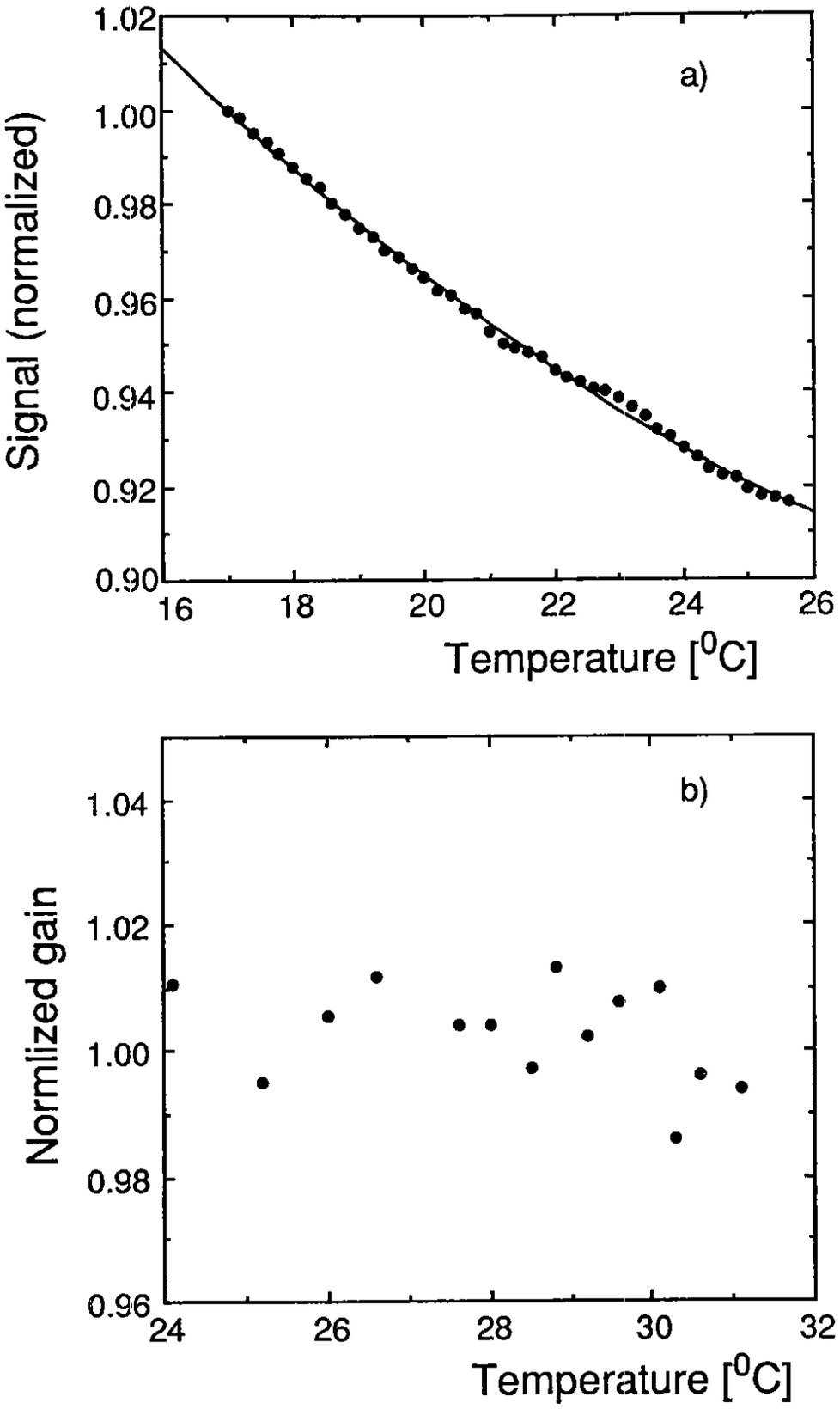
a)
Signal (normalized)
1.02
1.00
0.98
0.96
0.94
0.92
0.90
16
18
20
22
24
26
Temperature [^{0}C]
b)
Normlized gain
1.04
1.02
1.00
0.98
0.96
24
26
28
30
32
Temperature [^{0}C]

Fig. 14.

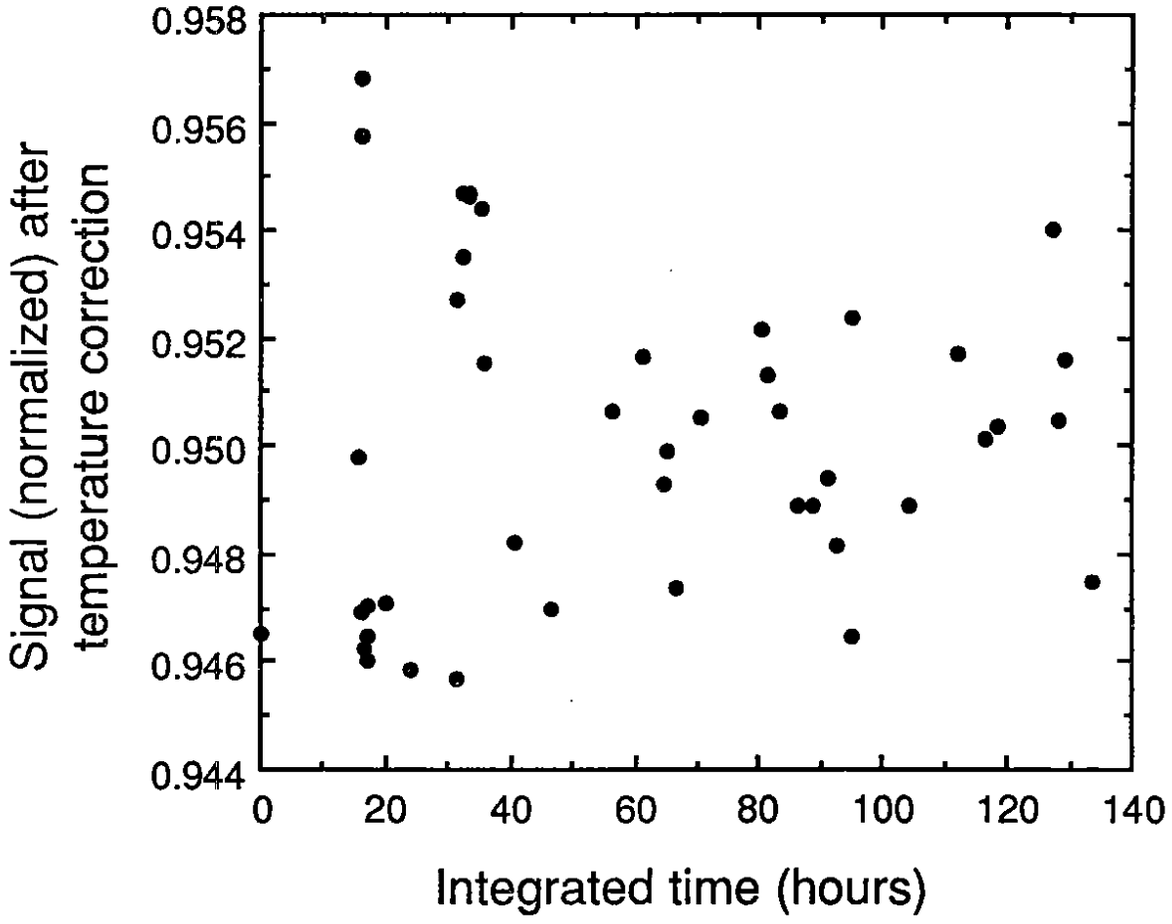
Signal (normalized) after temperature correction
0.958
0.956
0.954
0.952
0.950
0.948
0.946
0.944
0
20
40
60
80
100
120
140
Integrated time (hours)

Fig. 15.

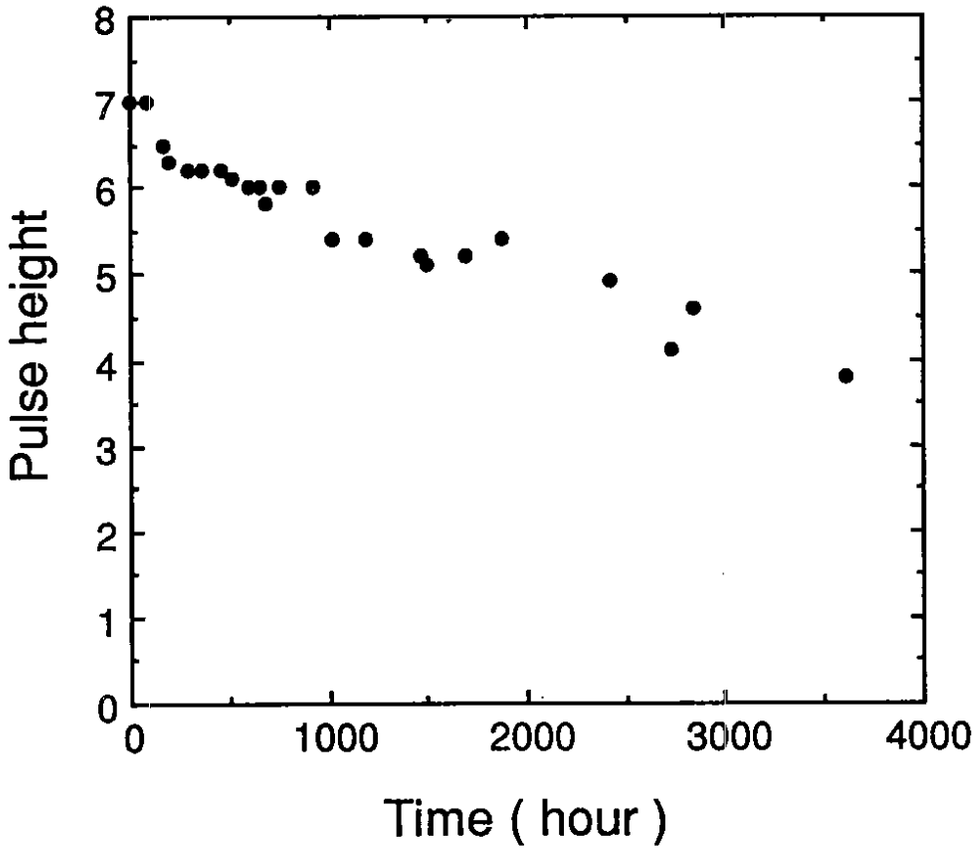

Fig. 16.

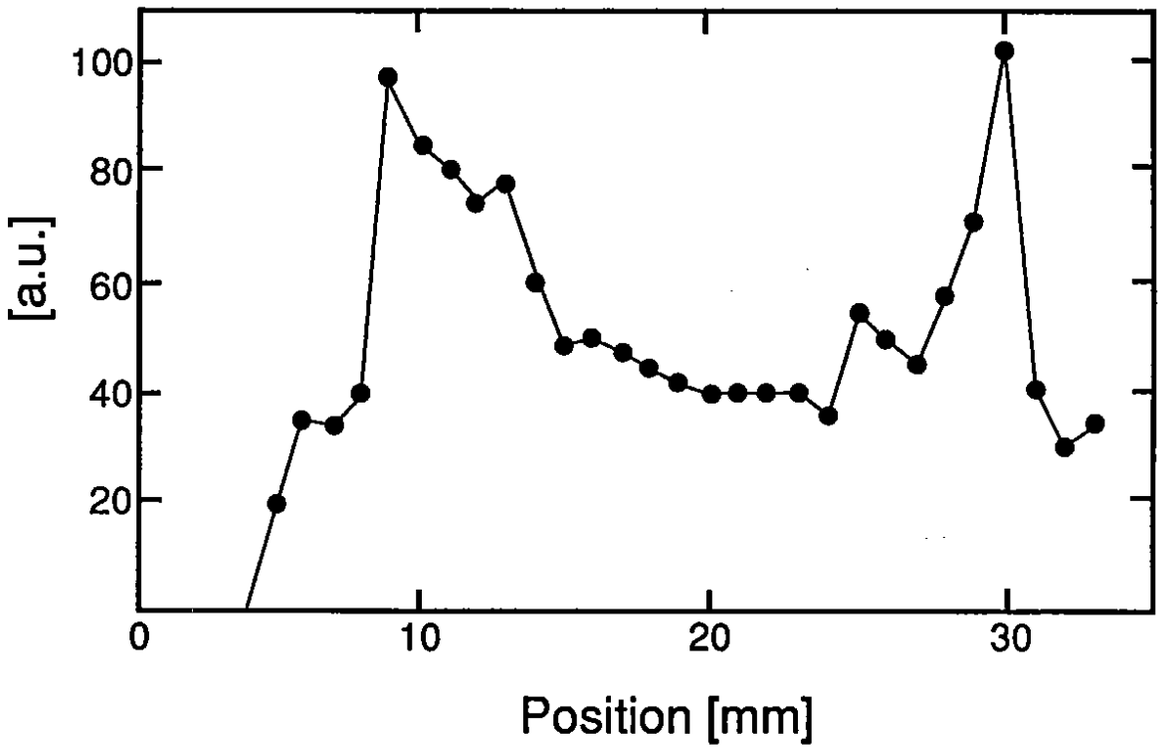

Fig. 17.

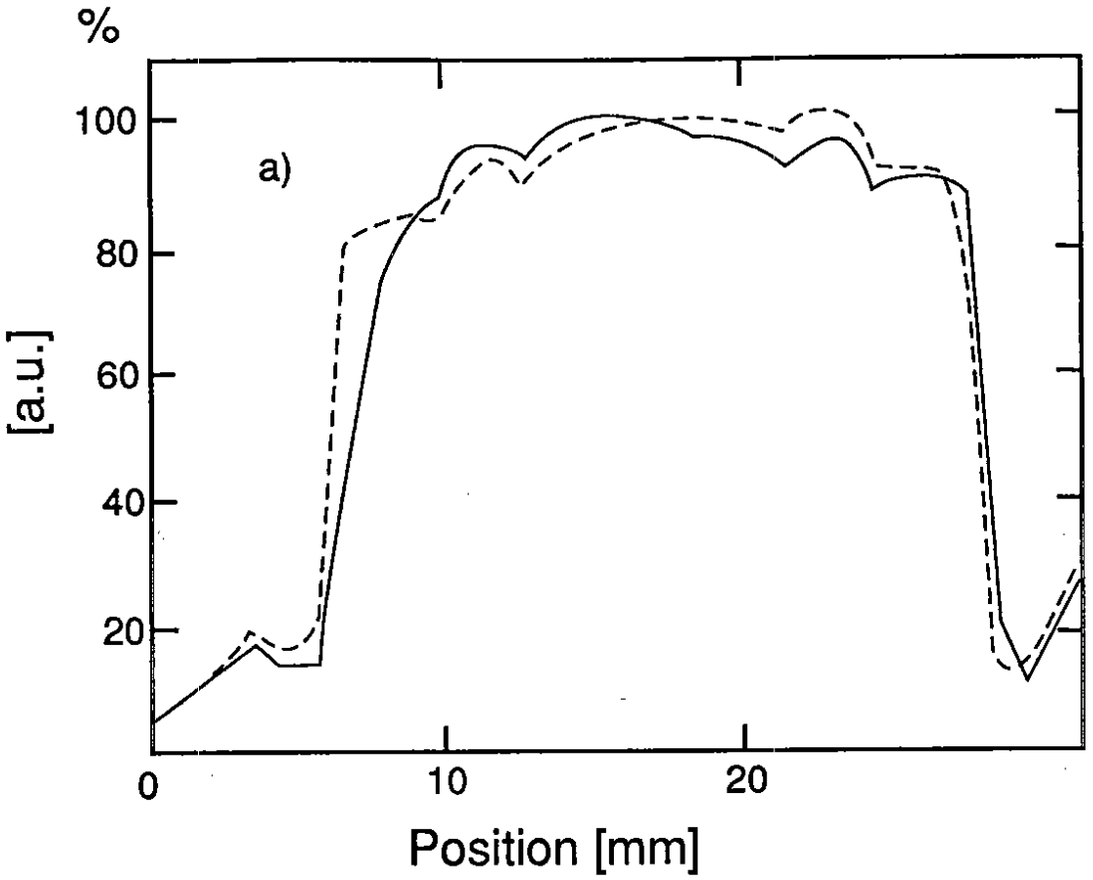
%
100
80
60
40
20
[a.u.]
a)
0
10
20
Position [mm]

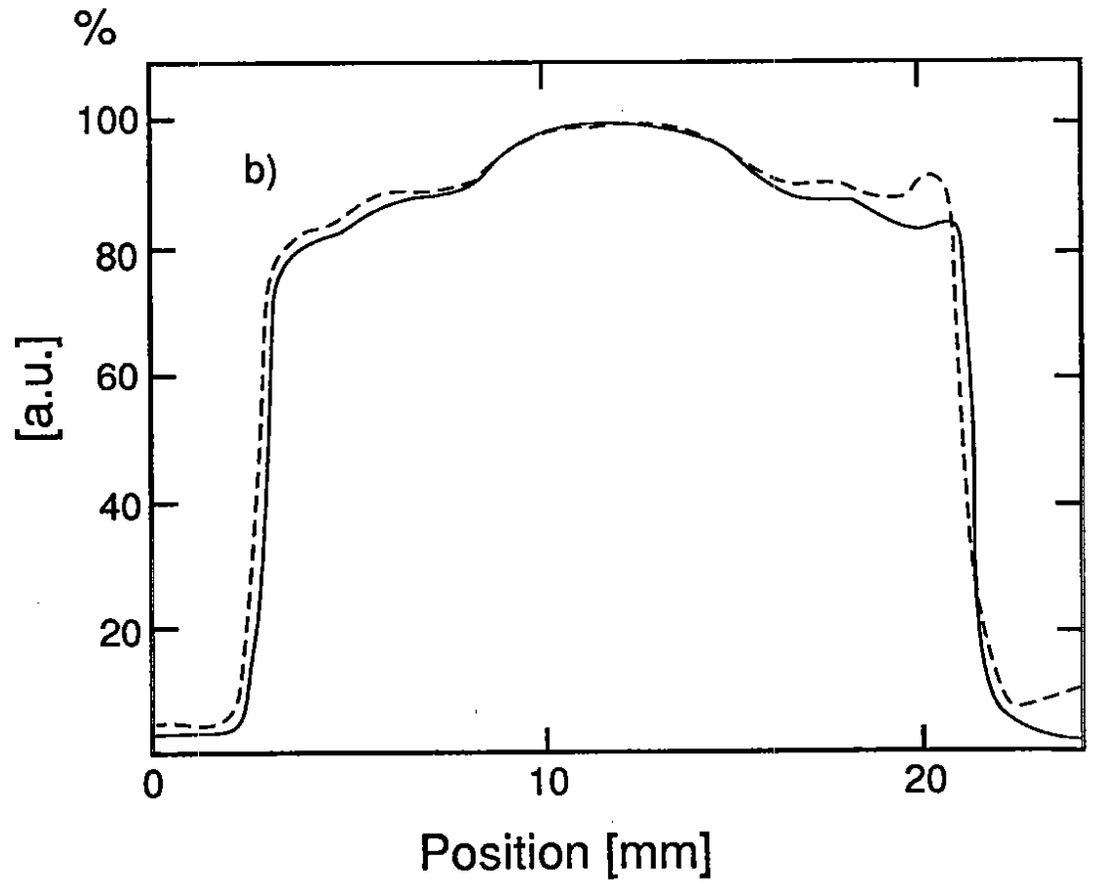
%
100
80
60
40
20
[a.u.]
b)
0
10
20
Position [mm]

Fig. 18.

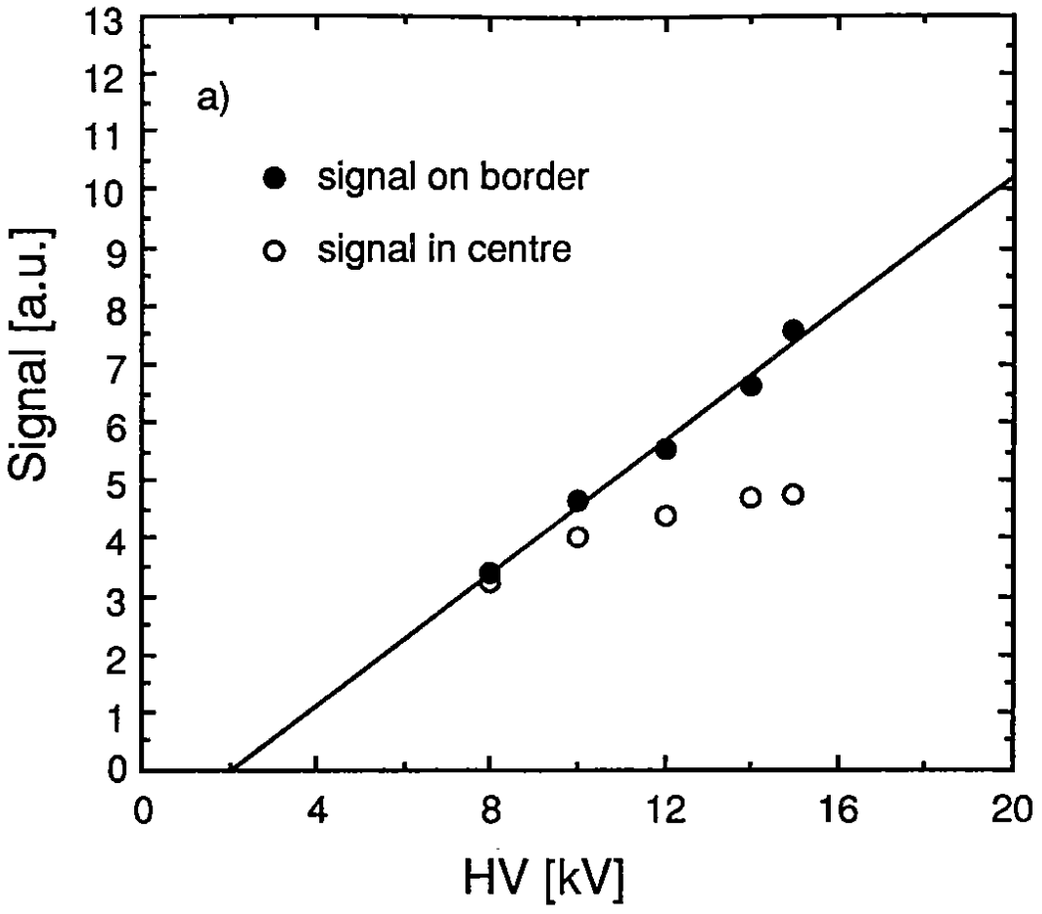
a)
signal on border
signal in centre
Signal [a.u.]
HV [kV]
0
1
2
3
4
5
6
7
8
9
10
11
12
13
0
4
8
12
16
20

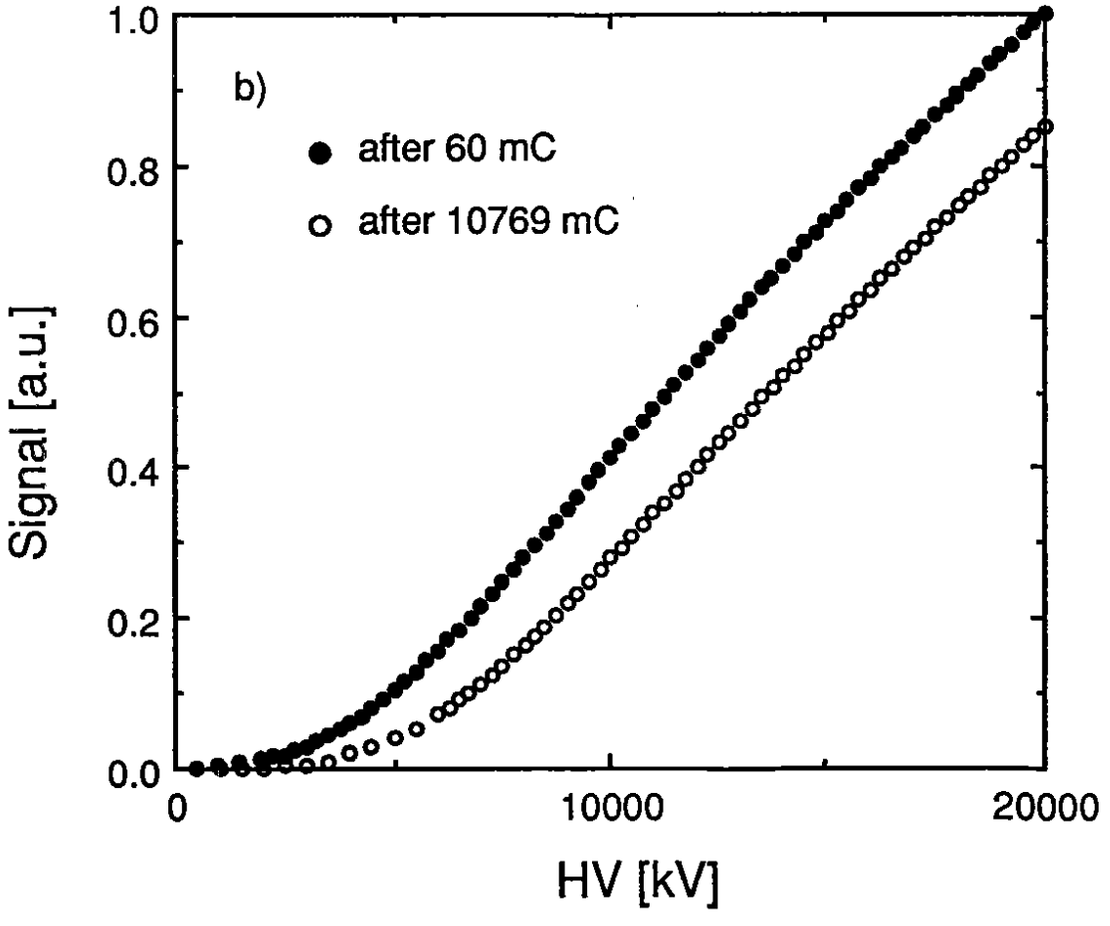
b)
after 60 mC
after 10769 mC
Signal [a.u.]
HV [kV]
0.0
0.2
0.4
0.6
0.8
1.0
0
10000
20000

Fig. 19.

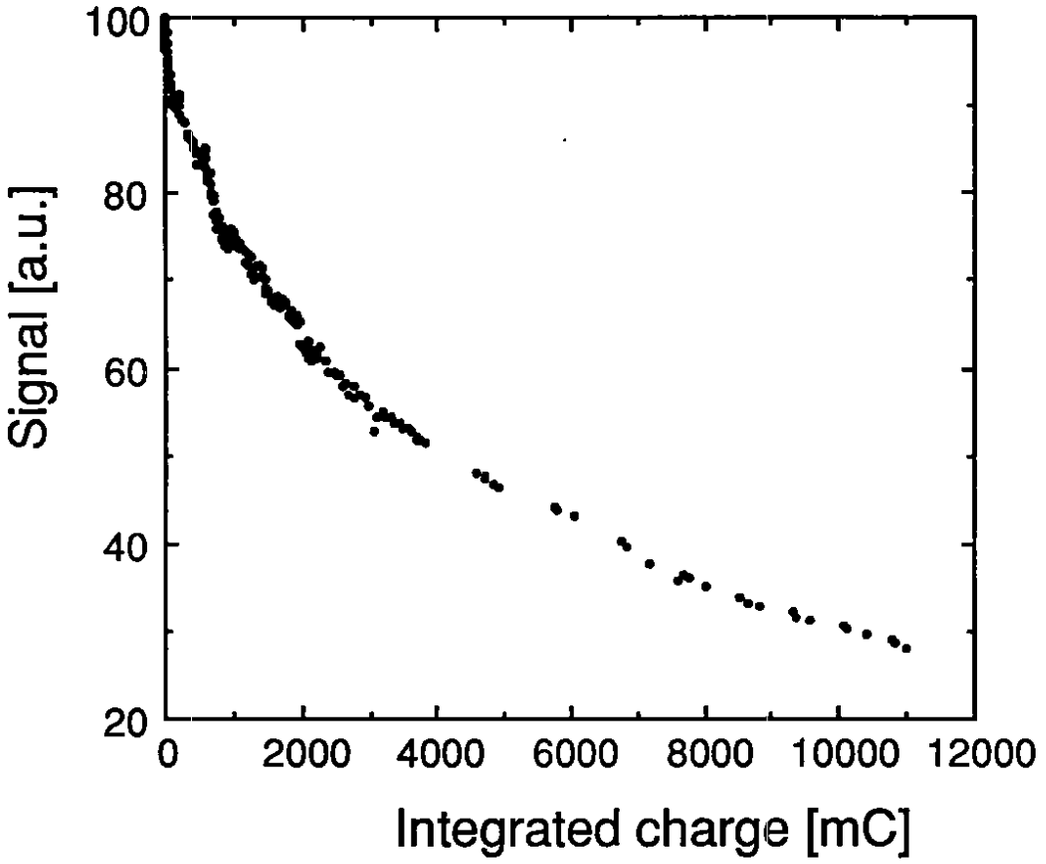
100
80
60
40
20
Signal [a.u.]
0
2000
4000
6000
8000
10000
12000
Integrated charge [mC]

Fig. 20.

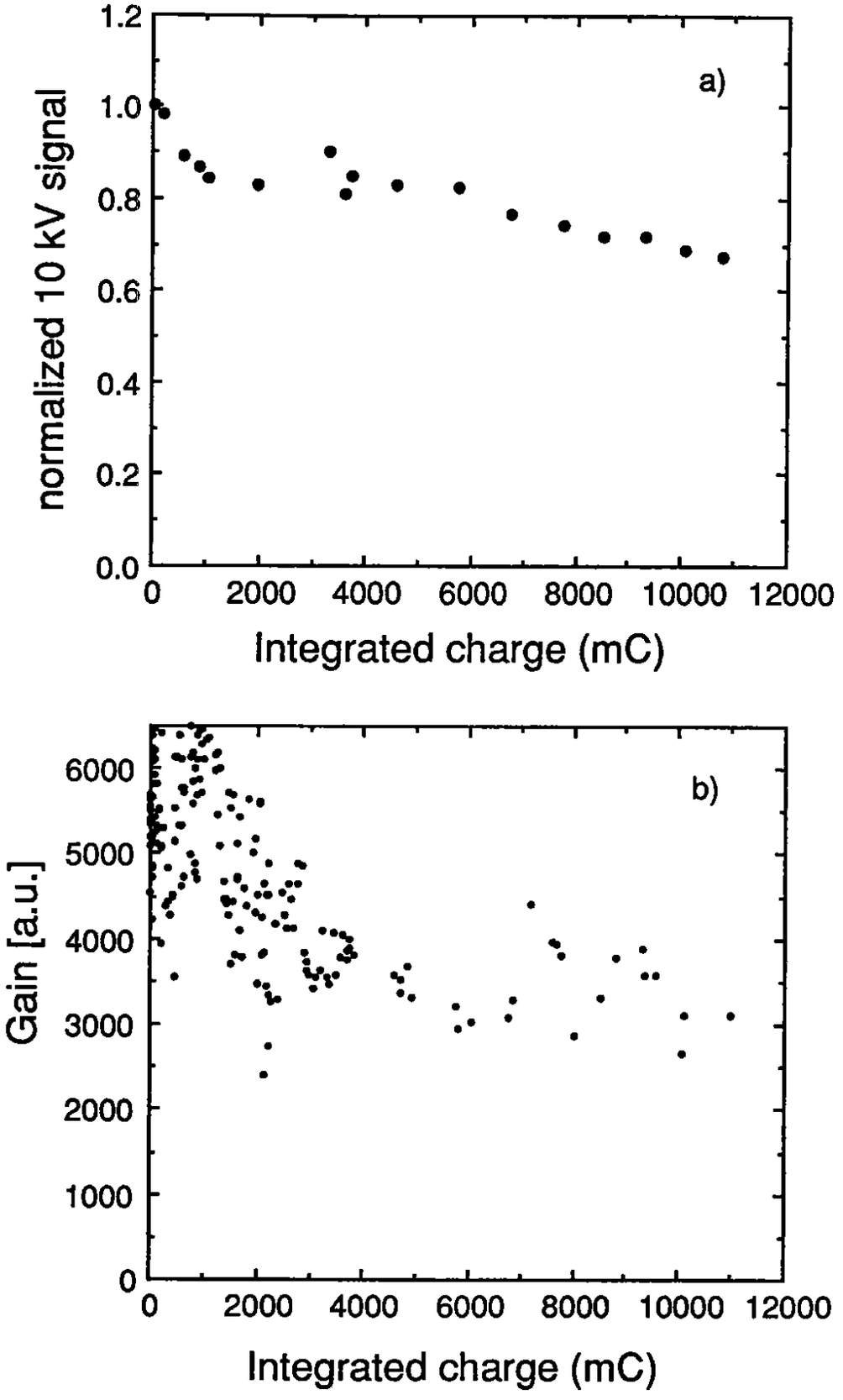
a)
normalized 10 kV signal
1.2
1.0
0.8
0.6
0.4
0.2
0.0
0
2000
4000
6000
8000
10000
12000
Integrated charge (mC)
b)
Gain [a.u.]
6000
5000
4000
3000
2000
1000
0
0
2000
4000
6000
8000
10000
12000
Integrated charge (mC)

Fig. 21.